Optimal beam diameter for lateral optical forces on microspheres at a water-air interface

Mincheng Zhong (钟敏成), Xi Wang (王 茜), Jinhua Zhou (周金华), Ziqiang Wang (王自强), and Yinmei Li (李银妹)*

Department of Optics and Optical Engineering, Anhui Key Laboratory for Optoelectronic Science and Technology, University of Science and Technology of China, Hefei 230026, China

**Corresponding author: liyinmei@ustc.edu.cn*

Received August 26, 2013; accepted November 28, 2013; posted online January 8, 2014

Optical tweezers with a low numerical aperture microscope objective is used to manipulate the microspheres at the water-air interface. In this letter, we determine the optimal optical trap for the lateral manipulation of microspheres at a water-air interface. The experimental results show that the trapping force is influenced by the expansion of the trapping beam at the back aperture of the objective. The optimal filling ratio of 0.65 is suggested for lateral optical manipulation at the water-air interface. The lateral trapping forces at the water-air interface are theoretically investigated with the ray-optics model. The numerical results show that the lateral trapping forces can be changed by shrinking the diameter of the trapping laser beam. The numerical results are in accordance with the experimental results.

OCIS codes: 140.7010, 170.4520, 080.5692.
doi: 10.3788/COL201412.011403.

Optical tweezers[1] have various applications such as manipulation and sorting of small particles[2−9]. In most of these applications, three-dimensional (3D) trapping is always performed in a liquid environment. Furthermore, optical tweezers can be used to trap colloidal particles at a liquid-liquid interface[10,11] or a liquid-air interface[12,13]. In such applications, optical tweezers should be optimized to reduce local heating and diminish the power of trapping laser, which causes a surface tension variation at the surface[14].

One of important parameters in the optimization of optical tweezers is the filling factor W/D[15−17], in which W and D are the beam spot diameter (the diameter at which the intensity decreases to $1/e^2$ of the central value) and the diameter of the objective's entrance aperture, respectively. Samadi *et al.*[16] have shown that W/D=0.67 provides the strongest lateral trap stiffness for a micrometer-sized bead in the water. Meng *et al.*[18], suggested that a W/D of 0.6−0.72 is optimal for optical tweezers in force-measurement applications. Given that 3D trapping requires mainly the axial confinement of particles, a high numerical aperture (NA) objective should be used in the optical tweezers setup. When particles are trapped at the water-air interface, the axial optical force can be neglected because it is too small to overcome the capillary force. However, analysis of the optimized W/D for optical manipulation at the liquid-air interface has not yet been thoroughly investigated. In this letter, we investigate the optimal W/D to improve the optical trapping force at the water-air interface.

Our optical tweezers setup is based on an Olympus IX70 inverted microscope, as sketched in Fig. 1. The microscope is a universal infinity corrected optical system. A linearly polarized He–Ne laser with 35-mW output power is used as the trapping laser source. This laser beam is expanded by a beam expander (BE). The beam diameter is controlled by different–sized holes (H). Lens L1 (f = 250 mm) is placed after the hole and focuses the laser beam onto the conjugate point of the microscope objective (Fig. 1) after the beam is reflected by mirrors M1 and M2. The laser beam is then directed into the microscope, reflected upward with a dichroic mirror (DM), and refocuses into a sample chamber after passing through lens L2 (L2 is the tube lens inside the microscope, f = 180 mm) and a microscope objective (MO; 60×, NA = 0.7, diameter of back entrance = 6 mm, Olympus, Japan). The W values at the back aperture of the objective are changed by adjusting the hole size. The motion of particles are detected with a charge-coupled device (CCD) camera. The sample stage is driven by a 3D piezoelectronic transducer (PZT) (P-517.3CL, PI, German). The drift of the objective is compensated by adjusting the sample height axially using the PZT transducer.

The sample is a diluted suspension of 5-μm polymer particles (Duke Scientific, 4205A, USA). The water-air interface is prepared using a homemade, circular trough with an inner diameter of 10 mm and height of 1 mm. About 40 μL of diluted suspension is injected into the trough and sealed with two coverslips. The height of the water–air interface is about 500 μm, in which the microscope objective can work.

Optical tweezers with a low NA objective are unable to trap particles in water because the scattering force is larger than the gradient force. In our experiment, the particles in water are pushed to the water-air interface

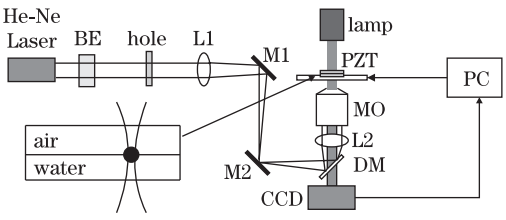

Fig. 1. Schematic of the experimental setup.

by the scattering force. Upon reaching the interface, the particles are located by surface tension. Thus, optical tweezers can manipulate the particles at the two-dimensional (2D) interface without stable axial optical confinement. The particles at the focus center can be tightly trapped when it is at the water–air interface. The optical trapping of particles at the water–air interface is shown in the Fig. 2. The trapped particle is stationary, whereas the other particles are moved by the PZT transducer.

The stability of optical trapping at the interface is important to colloidal-interaction applications. The effect of trapping stiffness on trapping depth can be neglected because the trapping depth is so large in our experiment. The main influence impactor is the thermal effect of the laser at the interface. Accordingly, we investigate the variation of optical force with time to check the stability of optical trapping at the interface. The trapping force is qualitative with critical escape velocity. The piezoelectric transducer is driven by a triangle wave of variable frequency and amplitude; hence, the trapped particle is forced to move back and forth relative to the surrounding liquid at constant speed. The viscous force that the particle endures can be quantitatively controlled by changing the frequency and amplitude of the triangle wave. When the drag force is large enough, the particle escapes from the trap. The critical escape drag force can characterize the maximal trapping force. The experimental results in Fig. 3 show that the lateral optical force on the particles at the interface is stable within 30 min. The symbols in Fig. 3 indicate the average of five experimental measurements for each time, whereas the error bars indicate statistical errors.

We perform experiments with different beam diameters (W) at back entrance of a microscope objective to determine the optimal W/D for lateral trapping at the water-air interface. The initial laser beam is expanded up to 6 mm at the back aperture of the trapping microscope. The beam diameter W is adjusted using a series of circular holes with different diameters, and the laser power is measured with a power meter (Labmaster, Coherent, USA).

The beam has a Gaussian intensity distribution at the position of the exit pupil, and the $I(r)$ at a distance r from the beam axis can be given as

$$I(r) = I_0 \exp(-2r^2/\omega_0^2), \tag{1}$$

where w_0 is the waist of the laser beam, and I_0 is the intensity at the center of the laser beam. The transmissivity T of holes for the power P is $T = P/P_{\text{total}} = 1-\exp(-2a^2/\omega^2)$, where a is the radius of the hole. Thus, the waist of beam w after the hole is

$$w = (-2a^2/\ln(1-T))^{1/2}. \tag{2}$$

The trapping force per laser power for different W/D values is presented in Fig. 4. The symbols indicate the average of five experimental measurements for each filling ratio, whereas the error bars are statistical errors obtained from a single measurement. The open circles represent the measurements of the particles at the interface. The maximum lateral trapping force for the particle in water is also presented in Fig. 4 for comparison. Results show an optimal $W/D \approx 0.65$, at which the strongest lateral trap appears. This value well agrees with the value when the particles are immersed in water. Generally, the trapping beam is always expanded to overfill the back aperture of the trapping objective, but previous study[16,18] has shown that the optimal lateral trapping is not gained when the back aperture is overfilled with the trapping laser. Our results confirm these previous results. The experiment in this letter is more intuitional because the particles are located at the water-air interface and the influence of axial trapping force is excluded.

We calculate the trapping forces on the particle at the water-air interface using a ray-optics model with ray-tracing methodology[15,19]. In a typical procedure, the incident beam is decomposed into individual rays, and the effect of diffraction is neglected. The interactions between a particle at the water-air interface and a single ray are shown in Fig. 5(a). The coordinate is based on

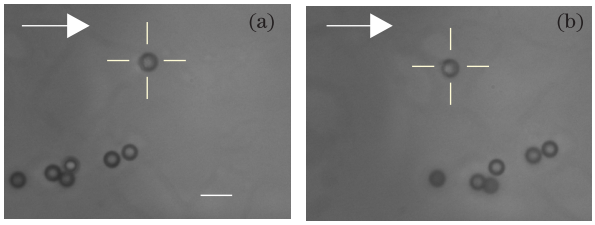

Fig. 2. Optical trapping of a single 5-μm polystyrene microsphere at the water–air interface. The white arrow indicates fluid flow. "+" indicates the center of the optical trap. Bar=10 μm.

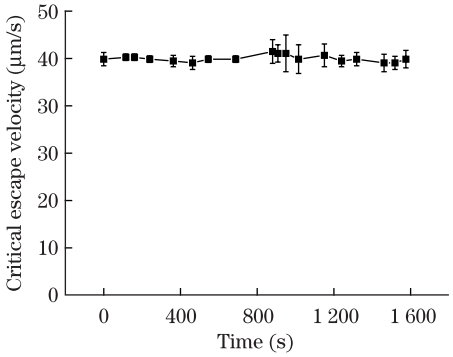

Fig. 3. Critical escape velocity versus time. The experiment is performed within 30 min.

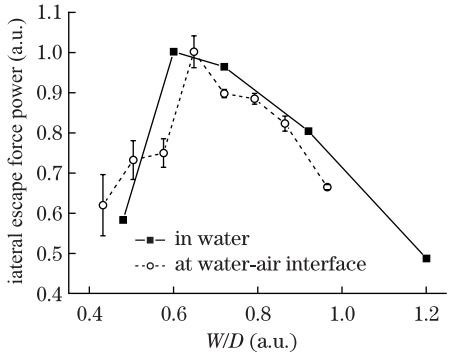

Fig. 4. Maximal lateral optical force versus filling ratio. The open circles represent the measurements of particles at the interface. The filled squares represent the measurements of particles in water.

the focus of an objective lens, the z-axis is along the beam axis, and the objective focus is set as the origin. The unit vector $\boldsymbol{u}$ indicates an incident ray from the objective lens given by $\boldsymbol{u} = (\sin\theta\cos\varphi, -\sin\theta\sin\varphi, \cos\theta)$, where θ is the angle between the z-axis and incident ray, and φ is the angle between the x-axis and the orthogonal projection of $\boldsymbol{u}$ to the incident plane. At the point of incidence P_1, the incident ray is decomposed into two rays: a transmitted ray and a reflected ray. The radiation force caused by reflection and refraction at point P_1 can be expressed as

$$\boldsymbol{f}_1(\theta,\varphi) = \frac{nP(r)}{c}(\boldsymbol{u}_1 - R_1\boldsymbol{v}_1 - T_1\boldsymbol{w}_1), \tag{3}$$

where n is the refractive index of surrounding medium determined by the location of point P_1, R_1 and T_1 are the reflectivity and transmissivity at point P_1, respectively; $\boldsymbol{v}_1$ and $\boldsymbol{w}_1$ are the unit vector of the reflected and refracted ray, respectively; c is the velocity of light in free space; $P(r)$ is the laser power at a distance r from the beam axis. The refracted part of the ray $T_1\boldsymbol{w}_1$ as a new incident ray reaches the next point P_2 on the surface, and the radiation force at P_2 can be similarly obtained by Eq. (3). The reflected ray repeatedly reflects and refracts at interaction points P_i with losing intensity. The radiation force for a single ray $\boldsymbol{f}$ is the summation of $\boldsymbol{f}_i$, and the radiation force $\boldsymbol{F}$ can be obtained by integrating over $\boldsymbol{f}$ for all incident rays emitted from the objective lens.

In our calculation, the refractive indices of the latex particles, water, and air are 1.55, 1.33, and 1, respectively, and the laser wavelength is 633 nm. The NA of the microscope objective is 0.7. Given the surface tension, about two–thirds of the particle (by diameter) is immersed in water, and the remaining one–third is in air[20]. The beam is assumed to have a Gaussian intensity distribution at the position of the exit pupil. The intensity of the s polarized component is equal to the intensity of the p polarized component in this calculation.

We present the calculated results in terms of trapping efficiency Q given by $F = nPQ/c$, where n is the refractive index of the surrounding medium (normalized by refractive index of water in the calculation result). The absolute value of Q_x on the particles at the interface is larger than those in water when the filling ratio is the same, as shown in Fig. 5(b). The refractive index of air is smaller than that of water, so the total momentum transferred from the laser beam to the particle increases, which adds to the trapping forces at the interface.

The lateral components of trapping efficiency Q_x are shown in Fig. 5(b). It can be seen that the absolute value of Q_x increases with decreased filling ratio. When the filling ratio is lower than 0.6, the diameter of the laser beam is very small, and the lateral trapping forces cannot be calculated with the ray optics model again. The lateral trapping force can be neglected when the laser beam is very small. We believe that an optimal filling ratio between 0 and 0.6 exists, and the experimental results show that the optimal filling ratio is about 0.65 at the interface. The difference in optimal filling ratio between the numerical simulation result and experimental result can be due to the accuracy of ray–optics model.

In conclusion, we investigate the optimal lateral optical trapping for the microspheres at the water–air interface. The lateral optical forces versus the filling ratio are obtained when the particles are at the water–air interface. Experimental results show that the expansion of the trapping beam at the back aperture of the objective influences the lateral trapping force. The lateral trapping forces at the interface are also numerically investigated with the ray–optics model. The numerical results are in accordance with the experimental results. The optimal filling ratio of 0.65 is suggested for lateral optical manipulation at the water–air interface according to the experiment results. We believe that the results are helpful in manipulating the particles and studying the property of colloidal particles at liquid interfaces.

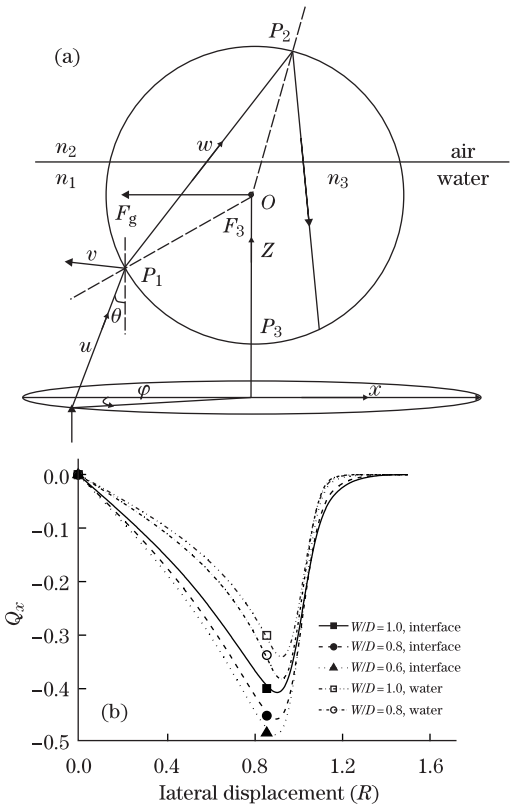

Fig. 5. Calculation of optical trapping forces on dielectric spheres with the ray-optics model. (a) Geometry for calculating the optical trapping force exerted on a particle located at a water-air interface by a single incident ray. (b) Lateral trapping efficiency versus the lateral displacement from the trapping center for different filling ratios.

This work was supported by the National Natural Science Foundation of China (Nos. 21073174 and 11302220) and the Key Laboratory of Microgravity, Institute of Mechanics, Chinese Academy of Sciences.

References

1. A. Ashkin, J. M. Dziedzic, J. E. Bjorkholm, and S. Chu, Opt. Lett. **11,** 288 (1986).
2. M. C. Zhong, X. B. Wei, J. H. Zhou, Z. Q. Wang, and Y. M. Li, Nature Commun. **4,** 1768 (2013).
3. R. W. Bowman, G. M. Gibson, M. J. Padgett, F. Saglimbeni, and R. Di Leonardo, Phys. Rev. Lett. **110,** 095902 (2013).

4. M. Zhong, G. Xue, J. Zhou, Z. Wang, and Y. Li, Chin. Opt. Lett. **10,** 101701 (2012).
5. K. Xiao and D. G. Grier, Phys. Rev. E **82,** 051407 (2010).
6. Y. Pang and R. Gordon, Nano Lett. **12,** 402 (2012).
7. T. Tao, J. Li, Q. Long, and X. Wu, Chin. Opt. Lett. **9,** 120012 (2011).
8. J. Yu, X. Tong, C. Li, Y. Huang, and A. Ye, Chin. Opt. Lett. **11,** 091701 (2013).
9. C. Wen and A. Ye, Chin. Opt. Lett. **11,** 091702 (2013).
10. R. Aveyard, B. P. Binks, J. H. Clint, P. D. I. Fletcher, T. S. Horozov, B. Neumann, V. N. Paunov, J. Annesley, S. W. Botchway, D. Nees, A. W. Parker, A. D. Ward, and A. N. Burgess, Phys. Rev. Lett. **88,** 246102 (2002).
11. B. J. Park, J. P. Pantina, E. M. Furst, M. Oettel, S. Reynaert, and J. Vermant, Langmuir **24,** 1686 (2008).
12. A. Jesacher, S. Furhapter, C. Maurer, S. Bernet, and M. Ritsch-Marte, Opt. Express **14,** 6342 (2006).
13. C. K. Sun, Y. C. Huang, P. C. Cheng, H. C. Liu, and B. L. Lin, J. Opt. Soc. Am. B **18,** 1483 (2001).
14. R. Dasgupta, S. Ahlawat, and P. K. Gupta, J. Opt. A: Pure Appl. Opt. **9,** S189 (2007).
15. M. Zhong, J. Zhou, and Y. Li, Chin. Opt. Lett. **8,** 673 (2010).
16. A. Samadi and S. S. Reihani, Opt. Lett. **35,** 1494 (2010).
17. M. Mahamdeh, C. Perez Campos, and E. Schaffer, Opt. Express **19,** 11759 (2011).
18. B. H. Meng, J. H. Zhou, M. C. Zhong, Y. M. Li, J. G. Wu, and H. L. Ren, Chin. Phys. Lett. **25,** 2300 (2008).
19. J. H. Zhou, H. L. Ren, J. Cai, and Y. M. Li, Appl. Opt. **47,** 6307 (2008).
20. W. Chen, S. S. Tan, Z. S. Huang, T. K. Ng, W. T. Ford, and P. Tong, Phys. Rev. E **74,** 021406 (2006).